

Review

Constraints on Theoretical Predictions Beyond the Standard Model from the Casimir Effect and Some Other Tabletop Physics

Galina L. Klimchitskaya ^{1,2}

¹ Central Astronomical Observatory at Pulkovo of the Russian Academy of Sciences, Saint Petersburg, 196140, Russia

² Institute of Physics, Nanotechnology and Telecommunications, Peter the Great Saint Petersburg Polytechnic University, Saint Petersburg, 195251, Russia

Received: 4 February 2021; Accepted: 23 February 2021; Published: 26 February 2021

Abstract: We review the hypothetical interactions predicted beyond the Standard Model which could be constrained by using the results of tabletop laboratory experiments. These interactions are described by the power-type potentials with different powers, Yukawa potential, other spin-independent potentials, and by the spin-dependent potentials of different kinds. In all these cases the current constraints on respective hypothetical interactions are considered which follow from the Casimir effect and some other tabletop physics. The exotic particles and constraints on them are discussed in the context of problems of the quantum vacuum, dark energy, and the cosmological constant.

Keywords: Casimir effect; hypothetical interactions; power-type potentials; Yukawa-type potential; spin-dependent potentials; constraints on hypothetical particles

1. Introduction

Despite great successes of the Standard Model, there is general agreement that it does not provide a solution to a number of crucial problems of modern physics such as quantization of the gravitational field [1], the enormously large energy density of the quantum vacuum [2], strong CP violation in QCD [3], the problems of dark matter and dark energy [4], etc. In attempting to solve these fundamental problems in the framework of the extended Standard Model, supersymmetry, supergravity and string theory, a lot of hypothetical interactions and elementary particles have been introduced which are characterized by a very weak interaction with particles of the Standard Model and cannot be detected using the present day accelerator techniques.

Among these particles are the massless pseudoscalar Goldstone bosons arions [5], light pseudo Nambu-Goldstone bosons axions [6,7] which arise from violation of the Peccei-Quinn symmetry [8], spin-1 elementary excitations of the gravitational field in extra dimensions graviphotons [9], scalar particles dilatons (radions) which arise in the multidimensional schemes with spontaneously compactified extra dimensions [10], the Nambu-Goldstone fermions goldstinos introduced in the supersymmetric theories with a spontaneously broken supersymmetry [11,12], etc. During the last few years much attention was attracted to the self-interacting scalar particles chameleons having a variable mass which is smaller in the regions of small matter density (i.e., in the interstellar space) and larger in the regions of large matter density (e.g., on the Earth) [13]. In a similar manner, the scalar fields called symmetrons have aroused considerable interest whose coupling constant depends on the density of matter in the environment [14].

An exchange of light and massless particles between the microscopic constituents of macroscopic bodies results in initiation of the effective interaction potentials and forces which are additional to the previously known fundamental forces, i.e., the gravitational, electromagnetic, weak and strong interactions. Any new force of this kind independently of its origin is often called *the fifth force* [15]. There are different types of effective potentials describing the new forces. For instance, an exchange of massless hypothetical particles of different spins leads to the power-type potentials and forces which are inverse proportional to different powers of separation. Note that the power-type corrections to Newton's gravitational law also arise in multidimensional theories with noncompact but warped extra dimensions [16,17]. An exchange of light scalar particles leads to the most popular new forces of Yukawa type [15], whereas an exchange of one pseudoscalar particle between nucleons of two macrobodies leads to the spin-dependent effective potential [18–20]. The Yukawa-type corrections to Newtonian gravity accessible to observations are also predicted by the multidimensional theories with compact extra dimensions and relatively low compactification scale of the order of 1 TeV [21–24]. The more complicated spin-independent interactions originating from an exchange of two axions and other hypothetical particles have also been predicted (see, e.g., [19,20,25]).

As already noted, it is unlikely that the predicted new forces will be observed using the accelerator techniques. They lead, however, to some additional interactions between the closely spaced macroscopic bodies which contain a huge number of elementary constituents and, thus, could be searched for in the tabletop laboratory experiments. These are the gravitational experiments of Eötvös and Cavendish type, experiments on neutron scattering, magnetometer measurements, measuring the decay rates of hypothetical particles into photons in strong magnetic field, precision atomic physics, etc. (see the reviews [26–30]).

Starting from the pioneer paper [31], experiments on measuring the van der Waals and Casimir forces are successfully used for constraining the hypothetical forces of Yukawa type. The point is that at separations below a few micrometers between the test bodies the gravitational interaction becomes so small that even by the orders of magnitude larger additions to it are not experimentally excluded. Thus, when searching for some hypothetical force at so short separations, one needs to use another familiar background force whose deviations from its theoretical law could serve as an alarm that one more physical effect comes into play. The van der Waals and Casimir forces, which are caused by the zero-point and thermal fluctuations of the electromagnetic field, just form the background of this kind in the separation range from a nanometer to a few micrometers. Therefore, any precise measurement of these forces can be used to impose constraints on some hypothetical interaction relevant to the same range of separations.

This article reviews the laboratory constraints on various hypothetical particles and interactions beyond the Standard Model obtained from experiments on measuring the Casimir interaction and some other tabletop experiments which lead to constraints in the parameter regions neighboring to those covered by the Casimir effect. We start from constraints on the power-type interactions with different powers and continue with the interactions of Yukawa type which are often considered in the literature as corrections to Newton's law of gravitation at short separations. Next we deal with some other spin-independent effective potentials which describe an exchange of two axionlike particles and certain other processes. Special attention is given to the constraints on the spin-dependent interactions originating from an exchange of one axion and by several more exotic processes. Axions and axionlike particles are often considered as possible constituents of dark matter [27,29]. Constraints on the parameters of several exotic particles like chameleons, symmetrons and massive photons are also considered, as well as their implications to the problem of dark energy. In some cases not only the already obtained constraints are presented but various proposals, plans and suggestions allowing their strengthening are discussed as well. Note that many corrections to the Casimir force which are a priori

much smaller than the corrections due to nonideality of the plate metal are widely discussed in the literature (see, e.g., the corrections in theories with a minimal length [32] or in a static space-time with a Lorenz-violating term [33]). All these subjects are outside the scope of our review.

The article is organized as follows: In Sections 2 and 3 the interactions of the power and Yukawa type are considered, respectively. Section 4 is devoted to other spin-independent interactions. In Section 5, the constraints on spin-dependent interactions are discussed. Sections 6 and 7 deal with some exotic particles and their implications to the problems of quantum vacuum, dark energy and the cosmological constant. In Section 8 the reader will find the discussion and in Section 9 – our conclusions. We use the system of units where $\hbar = c = 1$.

2. The Hypothetical Interactions of Power Type

Potentials of the hypothetical interactions of power and Yukawa type are usually presented in the form of corrections to the Newtonian gravitational potential. Thus, the power-type corrections can be parametrized as

$$V_l(r) = V_N(r) \left[1 + \Lambda_l \left(\frac{r_0}{r} \right)^{l-1} \right], \quad V_N(r) = -\frac{Gm_1m_2}{r}, \quad (1)$$

where G is the gravitational constant, m_1 and m_2 are the two point masses (atoms, nucleons) spaced at the points \mathbf{r}_1 and \mathbf{r}_2 , $r = |\mathbf{r}_1 - \mathbf{r}_2|$, and Λ_l with $l = 1, 2, 3, \dots$ are the dimensionless constants characterizing the strength of the power-type interaction. The quantity r_0 is introduced to preserve the correct dimension of V_l . It is often chosen as $r_0 = 1 \text{ F} = 10^{-15} \text{ m}$. Note that (1) is unrelated to the post-Newtonian approach presenting the deviations of Einstein's general relativity theory from Newton's law in powers of some small parameter. Here, the correction to unity can be of nongravitational origin.

The effective potential (1) with $l = 1$ arises due to an exchange of one massless particle (the Coulomb-type potential). An exchange of two arions between electrons belonging to atoms of two neighboring macrobodies results in the power-type correction with $l = 3$ which decreases with separation as r^{-3} [34]. The power-type corrections to the Newtonian potential with higher powers result from an exchange of the even numbers of neutrinos, goldstinos, and other massless fermions. For instance, an exchange of the neutrino-antineutrino pair between two neutrons leads to the power-type correction with $l = 5$ which decreases with increasing separation as r^{-5} [35,36]. For the multidimensional models with noncompact extra dimensions at separations $r \gg 1/k$, where k is the warping scale, the effective potential takes the form of (1) with $l = 3$, $\Lambda_3 = 2/(3k^2r_0^2)$ [16,17].

The constraints on the interaction constants Λ_l with different l can be obtained from the Eötvös-type or Cavendish-type experiments. The presence of some hypothetical interactions in addition to the Newtonian gravitation would lead to a seeming difference between the inertial and gravitational masses, i.e., to a violation of the equivalence principle tested by the Eötvös-type experiments. Using this approach, the maximum values of $|\Lambda_1|$ and $|\Lambda_2|$ allowed by the short-range Eötvös-type experiments are the following:

$$|\Lambda_1|_{\max} = 1 \times 10^{-9} \text{ [37]}, \quad |\Lambda_2|_{\max} = 4 \times 10^8 \text{ [38]}. \quad (2)$$

We recall that even a confirmed difference of Λ_l from zero would not imply a violation of the equivalence principle if the correction term in (1) is of nongravitational origin.

As to the Cavendish-type experiments, they test deviations of the gravitational potential $V_{\text{gr}}(r)$ from Newton's law. These deviations can be quantified by the value of the dimensionless parameter

$$\delta = \frac{1}{V_{\text{gr}}(r)} \frac{\partial}{\partial r} [rV_{\text{gr}}(r)], \quad (3)$$

which is identically equal to zero if $V_{\text{gr}}(r) = V_N(r)$ defined in (1). On this basis, the maximum values of $|\Lambda_l|$ with $l = 2, 3, 4$ and 5 allowed by the Cavendish-type experiment performed in 2007 were found to be [39]

$$|\Lambda_2|_{\text{max}} = 4.5 \times 10^8, \quad |\Lambda_3|_{\text{max}} = 1.3 \times 10^{20}, \quad |\Lambda_4|_{\text{max}} = 4.9 \times 10^{31}, \quad |\Lambda_5|_{\text{max}} = 1.5 \times 10^{43}. \quad (4)$$

One should take into account that we have recalculated the results of [39] to our choice of r_0 (in [39] $r_0 = 1$ mm was used). As is seen from (2), the constraint on $|\Lambda_2|$ in (4) is slightly weaker than that one following from the Eötvös-type experiment [38].

In [34,40] it was suggested to constrain Λ_l using the measure of agreement between experiment and theory for the Casimir force measured in [41] in the configuration of a plate and a spherical lens. It was shown [34,40] that measurements of the Casimir force result in

$$|\Lambda_2|_{\text{max}} = 1.7 \times 10^{11}, \quad |\Lambda_3|_{\text{max}} = 8.5 \times 10^{23}. \quad (5)$$

These constraints are weaker than the constraints (2) and (4) following from the experiments of Eötvös and Cavendish type. In 1987, however, when the constraints (5) on $|\Lambda_2|$ and $|\Lambda_3|$ from the Casimir effect have been obtained, they were the strongest ones. In succeeding years there was some kind of competition between measurements of the Casimir force and gravitational experiments in obtaining the strongest constraints on $|\Lambda_l|$ with $l = 2$ and 3 [42,43].

The constraints on $|\Lambda_1|$ and $|\Lambda_2|$ in (2) and on $|\Lambda_l|$ with $l = 2, 3, 4$ and 5 in (4) following from the Eötvös- and Cavendish-type experiments were the strongest ones during the period from 2007 to 2020. In 2020 the new Cavendish-type experiment has been performed [44] providing an improved test of the Newton law at short separations. As a result, somewhat stronger constraints on $|\Lambda_l|$ with $l = 2, 3, 4$, and 5 than in (4) were obtained. In Table 1 we summarize the strongest current constraints on Λ_l .

Table 1. The strongest current constraints on the potentials of power type.

l	$ \Lambda_l _{\text{max}}$	Source
1	1×10^{-9}	[37]
2	3.7×10^8	[44]
3	7.5×10^{19}	[44]
4	2.2×10^{31}	[44]
5	6.7×10^{42}	[44]

The probability exists of further strengthening of the constraints of Table 1. By way of example, there are proposals in the literature to constrain the power-type hypothetical interactions of different origin at micrometer separations by means of optomechanical methods exploiting the levitated sensors [45] or using experiments on neutron scattering and molecular spectroscopy [46].

3. The Yukawa-Type Interactions

The potential of Yukawa type is commonly presented as a correction to Newtonian gravitation

$$V(r) = V_N(r) \left(1 + \alpha e^{-\frac{r}{\lambda}} \right), \quad (6)$$

where α is the dimensionless constant characterizing the interaction strength and λ is the interaction range. As mentioned in Section 1, the Yukawa-type correction to Newton's law arises due to an exchange of one light scalar particle of mass $m = 1/\lambda$ between atoms of two macroscopic bodies and

in multidimensional theories with compact extra dimensions which are compactified at the low energy scale. This motivated numerous experiments searching for the corrections of this kind.

When integrated over the volumes V_1 and V_2 of two test bodies spaced at a small distance a , the potential (6) results in the interaction energy of these bodies. Calculating the negative derivative of this energy with respect to a , one arrives to the force

$$F(a) = -\frac{1}{V_1 V_2} \frac{\partial}{\partial a} \int_{V_1} \int_{V_2} V(r) d^3 r_1 d^3 r_2. \quad (7)$$

At separations a below a few micrometers the contribution of the Newtonian gravity to (7) is usually negligibly small as compared to the sensitivity of force measurements.

As was noted in Section 1, at separations below a few micrometers the main background force acting between electrically neutral test bodies is the Casimir force caused by the zero-point and thermal fluctuations of the electromagnetic field [47]. In the beginning of the XXI century the Casimir force and its gradient were measured in many precision experiments (see [48] for a review). The measurement results were found in agreement with theoretical predictions of the fundamental Lifshitz theory in the limits of some errors. By assuming that the Casimir forces $F_C^{\text{expt}}(a_i)$ measured at the separations a_i agree with the theoretical predictions $F_C^{\text{theor}}(a_i)$ up to the errors $\Delta_i F_C$, i.e., that the inequality

$$\left| F_C^{\text{expt}}(a_i) - F_C^{\text{theor}}(a_i) \right| \leq \Delta_i F_C \quad (8)$$

is satisfied, one arrives at a conclusion that any additional force (7) must satisfy the condition

$$|F(a_i)| \leq \Delta_i F_C. \quad (9)$$

This condition imposes some constraints on the parameters α and λ of the Yukawa interaction defined in (6) and (7).

This approach, as mentioned in Section 1, was first used in [31] where the constraints on the Yukawa-type interaction were obtained from old measurements of the van der Waals force [41,49]. According to the results of [31], measurements of the van der Waals interaction place the strongest constraints on scalar particles with $m > 10^{-6}$ eV. This corresponds to the interaction range $\lambda < 20$ cm. At larger λ (smaller masses) the strongest constraints on the Yukawa interaction follow from gravitational experiments [31]. Below it is shown that modern experiments on measuring the Casimir force, as well as the new tests of the inverse-square law of gravity and equivalence principle, significantly modify these results.

During the last 20 years, many measurements of the Casimir force have been used to obtain constraints on the Yukawa-type interaction. Thus, in [50] the competitive constraints at small λ were found from measuring the Casimir force between two crossed cylinders [51]. These constraints have been further confirmed and strengthened in [52–54] using experiments on measuring the lateral and normal Casimir forces between sinusoidally corrugated surfaces [55–58] and the normal Casimir force in the configuration of a silicon carbide surface situated at only 10 nm separation from a sphere [59,60]. At larger λ strong constraints on the strength of Yukawa interaction α were obtained from measuring the effective Casimir pressure by means of micromechanical torsional oscillator [61–64]. These results were confirmed [65] using the experimental data of experiment on measuring the difference of Casimir forces [66]. Major progress in the field was reached by the so-called *Casimir-less* experiments which also measure the differential forces and are organized in such a way that the contribution of the Casimir force is completely nullified [67,68]. These experiments are especially sensitive to the presence of any additional interaction. The second of them [68] resulted in the most strong constraints over a wide

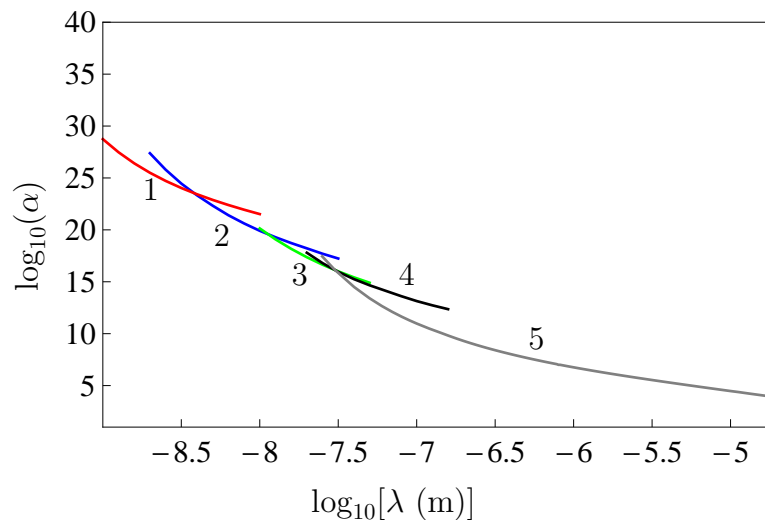


Figure 1. The strongest constraints on the Yukawa-type potentials obtained from measuring the Casimir force at nanometer separations (line 1), lateral Casimir force between corrugated surfaces (line 2), normal Casimir force between corrugated surfaces (line 3), the Casimir pressure (line 4), and from the Casimir-less experiment (line 5). The plane areas above the lines are excluded and below them are allowed by the measurement data.

interaction range. Much weaker constraints on α at relatively large λ were obtained in experiments using the torsion pendulum [69] and measuring the difference in the lateral forces [70].

In more detail, the above-listed experiments and constraints obtained from them are reviewed in [71]. In Figure 1, we present in the logarithmic scale only the strongest constraints on α for different $\lambda > 1$ nm obtained from measurements of the Casimir force. The line 1 is found [54] from [59,60], line 2 [52] from [55,56], line 3 [53] from [57,58], line 4 is obtained in [63,64], and line 5 in [68]. The (λ, α) -plane areas above each line are excluded by the measurement data of respective experiment and the plane areas below each line are allowed. To summarize, the line 1 presents the strongest constraints in the interaction region $1 \text{ nm} \leq \lambda < 3.7 \text{ nm}$, the line 2 in the region $3.7 \text{ nm} \leq \lambda < 11.6 \text{ nm}$, the line 3 in the region $11.6 \text{ nm} \leq \lambda < 17.2 \text{ nm}$, the line 4 in the region $17.2 \text{ nm} \leq \lambda < 40 \text{ nm}$, and the line 5 for $\lambda \geq 40 \text{ nm}$.

Similar to the power-type potentials, the potentials of Yukawa type are constrained by the results of Cavendish- and Eötvös-type experiments. The gravitational experiments are the most sensitive to the presence of additional interactions if the separation distance between the test bodies is sufficiently large so that gravitation remains to be the main background force. The most precise short-range Cavendish-type experiment of this kind was reported in [72]. For the interaction range of λ exceeding $8 \mu\text{m}$ the constraints on α following from [72] are stronger than those obtained in [68] from the Casimir physics. Thus, one can say that $\lambda = 8 \mu\text{m}$ (the respective mass of the hypothetical scalar particle is $m = 1/\lambda \approx 2.5 \times 10^{-2} \text{ eV}$) is the upper border of the current region of λ where the Casimir physics provides the strongest constraints on the Yukawa-type potentials. This means that during the period of time after 1987, when the possibility to constrain the Yukawa-type potentials from the Casimir effect was proposed [31], the role of gravitational and Casimir experiments in obtaining stronger constraints has vastly changed.

The constraints of [72] are the strongest ones up to $\lambda = 9 \mu\text{m}$. Within the wide interaction range from $\lambda = 9 \mu\text{m}$ to $\lambda = 4 \text{ mm}$ the strongest constraints on the Yukawa-type potentials follow [39] from another Cavendish-type experiment [73]. For even larger λ up to 1 cm the stronger constraints on α follow from an older Cavendish-type experiment [74] wherein the test masses were located at larger separations.

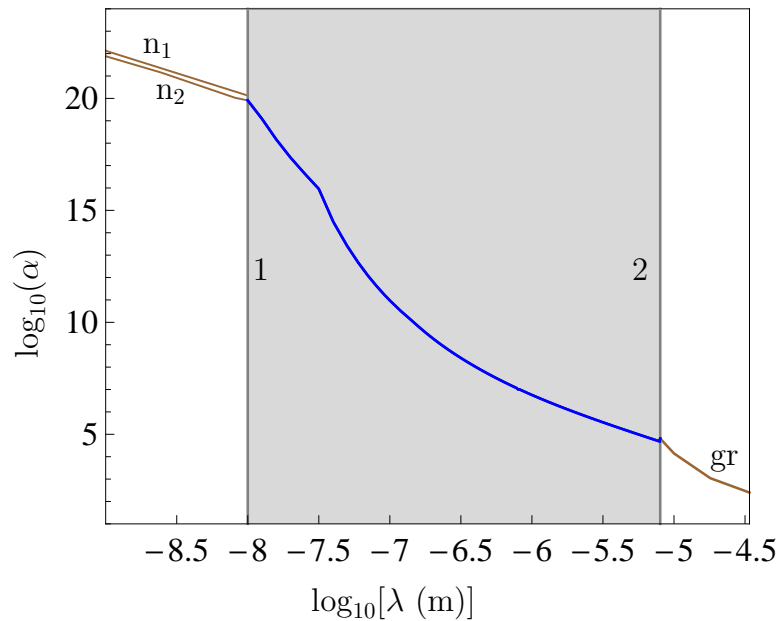


Figure 2. The strongest constraints on the Yukawa-type potentials obtained from two Cavendish-type experiments (line labeled "gr") and two experiments on neutron scattering (lines labeled "n₁" and "n₂"). The vertical lines labeled 1 and 2 indicate the current borders of the constraints obtained from Casimir physics. The latter are shown by the envelope curve in between the vertical lines 1 and 2. The plane areas above the lines are excluded and below them are allowed by the measurement data.

It should be mentioned also that in 2020 the constraints on α found in [73] were strengthened by up to a factor of 3 over the interaction range $40 \mu\text{m} \leq \lambda < 350 \mu\text{m}$ by refining the present techniques of Cavendish-type experiments [44] (as mentioned in Section 2, this experiment also leads to stronger constraints on the power-type potentials). For $\lambda > 1 \text{ cm}$ the best test for non-Newtonian gravity of Yukawa type is provided by the Eötvös-type experiments [38,75].

We illustrate the relative role of Casimir and gravitational experiments in strengthening the Yukawa-type interactions in Figure 2. The line marked gr in Figure 2 shows the constraints on the Yukawa-type potential from the Cavendish-type experiments [72,73]. In doing so, the constraints of the experiment [73] are shown from $\lambda = 9 \mu\text{m}$ to $\lambda = 34 \mu\text{m}$. The vertical line 2 at $\lambda = 8 \mu\text{m}$ indicates the current border between the strongest constraints on the Yukawa-type potentials obtained from gravitational experiments ($\lambda > 8 \mu\text{m}$) and from the Casimir effect ($\lambda \leq 8 \mu\text{m}$). At $\lambda \leq 8 \mu\text{m}$ in Figure 2 we plot the envelope curve of the strongest constraints on the Yukawa-type potentials from different Casimir experiments shown in Figure 1.

In the region of small λ the possibilities of Casimir physics in obtaining the strongest constraints on the Yukawa-type potentials are restricted by spectroscopic measurements in simple atomic systems like hydrogen or deuterium and scattering of slow neutrons on atoms. Thus, from the comparison of spectroscopic measurements with precise QED calculations it was found [76] that in the region $2 \times 10^{-4} \text{ nm} < \lambda < 20 \text{ nm}$ the interaction constant α varies from 2×10^{27} to 2×10^{25} . The strongest constraints in the interaction range around 1 nm were, however, obtained from two neutron experiments [77,78]. In Figure 2 these constraints are shown by the lines n₁ [77] and n₂ [78]. These constraints remain the strongest ones up to $\lambda = 10 \text{ nm}$ where they are replaced with the constraints from measurements of the lateral Casimir force between corrugated surfaces. Thus, the vertical line 1 in Figure 2 at $\lambda = 10^{-8} \text{ m}$

separates the constraints on the Yukawa-type potentials obtained from the neutron scattering and from the Casimir physics. Note that the constraints of [77,78] remain the strongest ones at $\lambda < 1$ nm as well (in the interaction region $0.03 \text{ nm} < \lambda < 0.1 \text{ nm}$ they have been further strengthened by the experiment using a pulsed neutron beam [79]).

One can conclude that at the moment Casimir physics provides the strongest constraints on the Yukawa-type potentials over the wide interaction range from $\lambda = 10^{-8} \text{ m}$ to $0.8 \times 10^{-5} \text{ m}$.

In the end of this section, we briefly discuss some suggestions on how the obtained constraints on the Yukawa-type potentials could be strengthened. Some improvements of the already performed experiments, which promise an obtaining up to one order of magnitude stronger constraints, were suggested in [80]. Along with experiments employing the sphere-plate geometry, the configurations of sinusoidally corrugated test bodies were considered. In this case the improvements in sensitivity can be reached by increasing the corrugation amplitudes and decreasing the corrugation period [80]. The levitated nanoparticle sensor, which is sensitive to static forces down to 10^{-17} N and could be helpful in constraining the Yukawa-type interactions, was proposed in [81]. In [82] it was argued that precision spectroscopy of weakly bound molecules can be used for sensing the non-Newtonian interactions between atoms. Calculations show that in the interaction range from $\lambda = 2 \text{ nm}$ to 10 nm this method allows to strengthen the constraints obtained from neutron scattering experiments by at least 1.5–2 orders of magnitude. The possibility to improve the constraints on α in the wide interaction region around $\lambda = 1 \text{ }\mu\text{m}$ by measuring the Casimir-Polder force in the configuration of a Rb atom and a movable Si plate with an Au film in between was proposed in [83]. Up to an order of magnitude stronger constraints on α in the interaction range from below a micrometer to $20 \text{ }\mu\text{m}$ is promised by the proposed CANNEX test (Casimir And Non-Newtonian force Experiment) which is adapted for measuring the Casimir pressure between two parallel plates at separations up to $10 \text{ }\mu\text{m}$ [84,85].

It should be noted that although the Yukawa-type corrections to the Newton gravitational law are short-ranged, they are important not only in the tabletop laboratory experiments but in astrophysics as well. For instance, as shown in [86], these corrections make an impact on the properties of quark stars and should be taken into account for interpretation of observations related to some specific events and objects.

4. Other Spin-Independent Hypothetical Interactions

The most popular spin-independent effective potential other than that of the Yukawa type originates from an exchange of two light pseudoscalar particles between two fermions under an assumption of the pseudoscalar coupling. This means that the Lagrangian density takes the form [87–89]

$$\mathcal{L}_P(x) = -ig\bar{\psi}(x)\gamma_5\psi(x)\varphi(x), \quad (10)$$

where $\psi(x)$ and $\varphi(x)$ are the spinor and pseudoscalar fields, respectively, γ_5 is the Dirac matrix and g is the dimensionless interaction constant.

Under a condition that $r \gg m^{-1}$, where r is the separation distance between two fermions and m is their mass, the effective potential of their interaction due to an exchange of two pseudoscalars takes the form [15,19,90]

$$V(r) = -\frac{g^4}{32\pi^3 m^2} \frac{m_a}{r^2} K_1(2m_a r), \quad (11)$$

where m_a is the mass of a pseudoscalar particle and $K_1(z)$ is the modified Bessel function of the second kind.

The most important hypothetical pseudoscalar particles are axions which were introduced [6,7] in order to solve the problems of strong CP violation and large electric dipole moment of neutron which

arise in quantum chromodynamics. The originally introduced axions are the Nambu-Goldstone bosons and their interaction with fermions is not described by (10) (see the next section). Later, however, some other types of axions (axionlike particles) were introduced, e.g., the so-called Grand-Unified-Theory (GUT) axions, which are coupled to fermions according to (10) [88]. Axions and axionlike particles are presently considered as the most probable constituents of dark matter and their search is underway in many laboratories all over the world (see [27,29,88,89] for a review).

In connection with this, much attention was recently attracted to the effective potential (11) which describes some additional force arising between two test bodies due to an exchange by the pairs of axions between their constituents. An interaction of two macrobodies by means of the two-axion exchange between their atomic electrons turned out to be too weak and does not lead to the competitive constraints on the axion-electron interaction. As to the interaction of axions with nucleons belonging to atomic nuclei, it leads to the competitive laboratory constraints on g in the wide range of axion masses m_a obtained from experiments on measuring the Casimir force and gravitational experiments (the stronger constraints obtained from astrophysics are of lesser reliability because the theory of dense nuclear matter is still not clearly understood [91]).

By integrating (11) over the volumes of two test bodies V_1 and V_2 and calculating the negative derivative of the obtained result, one obtains the additional force which arises due to the two-axion exchange between nucleons

$$F_{an}(a) = -\frac{m_a g^4}{32\pi^3 m^2} n_1 n_2 \frac{\partial}{\partial a} \int_{V_1} \int_{V_2} dr_1 dr_2 \frac{K_1(2m_a r)}{r^2}, \quad (12)$$

where $r = |\mathbf{r}_1 - \mathbf{r}_2|$ is a distance between nucleons belonging to V_1 and V_2 , and $n_{1,2}$ are the numbers of nucleons per unit volume of V_1 and V_2 (below we assume equal the coupling constants of an axion to a proton and a neutron). Then, similar to the interaction of Yukawa type, one can obtain constraints on m_a and g from the inequality

$$|F_{an}(a)| \leq \Delta_i F_C, \quad (13)$$

where $\Delta_i F_C$ is the measure of agreement between the experimental Casimir forces and theoretical predictions [compare with (8) and (9)].

The first constraints of this kind on the effective potential (11) and respective parameters of axionlike particles m_a and g were obtained [92] from measuring the Casimir-Polder force between the ^{87}Rb atoms and a silica glass plate [93]. Somewhat stronger constraints in the region of axion masses below 1 eV were found [94] from the experiment on measuring the gradient of the Casimir force between Au-coated surfaces of a sphere and a plate performed by means of an atomic force microscope [95]. All other Casimir experiments used for constraining the interaction of axionlike particles with nucleons are the same as already discussed in Section 3 in connection with constraining the Yukawa-type interaction. Thus, measurements of the effective Casimir pressure by means of micromechanical torsional oscillator [63,64] were applied for obtaining stronger constraints on axionlike particles in the region of axion masses $m_a \geq 1$ eV [96]. Measurements of the lateral Casimir force between sinusoidally corrugated surfaces [55,56] resulted in stronger constraints [97] for somewhat larger m_a than the constraints of [96] obtained from [63,64]. The most strong constraints in the range of axion masses $m_a < 1$ eV were obtained [98] from the second Casimir-less experiment [68]. These constraints were confirmed by slightly weaker independent constraints derived [65] from measuring the difference of Casimir forces [66]. Very recently, strong constraints on g in the region of axion masses up to $m_a = 100$ eV were obtained [54] from the experiment where the Casimir force was measured between a silicon carbide plate at 10 nm minimum separation from a metallic sphere [59,60].

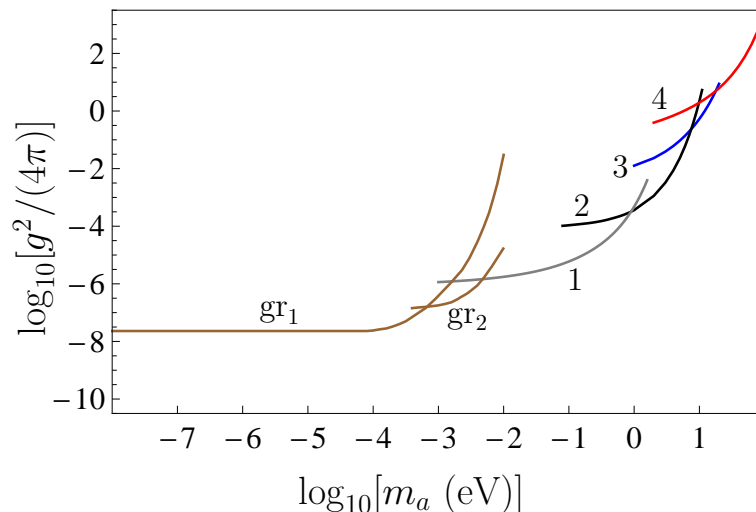


Figure 3. The strongest laboratory constraints on the coupling constant of axionlike particles to nucleons obtained from the Cavendish-type experiment (line labeled "gr₁"), from measuring the minimum forces of gravitational strength by means of torsion pendulum (line labeled "gr₂"), from the Casimir-less experiment (line 1), from measuring the Casimir pressure (line 2), lateral Casimir force (line 3), and the Casimir force at nanometer separations (line 4). The plane areas above the lines are excluded and below them are allowed by the measurement data.

Similar to the Yukawa-type correction to Newtonian gravity, the additional interaction caused by the effective potential (11) describing two-axion exchange leads to a difference between the inertial and gravitational masses and to deviations of the total force between two macrobodies from the inverse square law. This means that the presence of the force (12) can be tested in gravitational experiments. Following this line of attack, the constraints on g in the region of axion masses from $m_a \sim 10^{-8}$ eV to $m_a \sim 10^{-5}$ eV were obtained in [20] from the Eötvos-type experiment [38]. Somewhat stronger constraints in a wider range of axion masses were found [20] from the Cavendish-type experiments [74,99]. However, the strongest laboratory constraints on the coupling constant of axionlike particles to nucleons over the wide range of axion masses were obtained in [39] from the measurement results of more recent Cavendish-type experiment [73] which was already used in Section 3 for constraining the Yukawa-type interactions.

For slightly larger axion masses stronger constraints on g were obtained [25] from the experiment on measuring the minimum forces of gravitational strength using the planar torsional oscillators [100–102].

It should be recalled that the constraints on m_a and g following from the Casimir physics and from the experiments of Eötvos and Cavendish type are only appropriate for the GUT axions whose interactions with nucleons are described by the Lagrangian density (10). All these constraints are obtained using the effective potential (11) describing the two-axion exchange. Because of this, it is reasonable to consider the constraints of this type together.

In Figure 3 we present in the logarithmic scale the strongest constraints on the coupling constant g as a function of the axion mass m_a . The line labeled gr₁ is found [39] from the Cavendish-type experiment [73] and the line labeled gr₂ [25] from measuring the minimum forces of gravitational strength by means of the planar torsional oscillators [100–102]. The line 1 is obtained [98] from the Casimir-less experiment

[68], line 2 from measuring the effective Casimir pressure [63,64], line 3 [97] from measuring the lateral Casimir force between corrugated surfaces [55,56], and line 4 [54] from the experiment using a silicon carbide plate [59,60]. To summarize, the line gr_1 presents the strongest constraints on g in the region of axion masses $m_a < 0.676$ meV, the line gr_2 in the region $0.676 \text{ meV} \leq m_a < 4.9$ meV, the line 1 in the region $4.9 \text{ meV} \leq m_a < 0.9$ eV, the line 2 in the region $0.9 \text{ eV} \leq m_a < 8$ eV, the line 3 in the region $8 \text{ eV} \leq m_a < 17.8$ eV, and the line 4 in the region $m_a \geq 17.8$ eV.

From Figure 3, it remains unclear for how long one could continue the lines gr_1 and 4 to the left and to the right, respectively. The point is that in the range of smaller and larger axion masses the strongest constraints on g follow from some other types of laboratory experiments. They are sensitive to the process of one-axion exchange between two nucleons and, thus, lead to the spin-dependent effective potentials. Such kind of experiments are discussed in the next section where we finally determine the current region of axion masses in which the strongest constraints on g follow from the Casimir and gravitational experiments.

In the end of this section we briefly list some other spin-independent potentials which are under discussion in the literature. As an example, the spin-independent effective potentials between two massive spin-1/2 particles arising due to an exchange of two spin-0 or two spin-1 massive bosons were found in [25] in the cases of scalar (g_S), pseudoscalar (g_P), vector (g_V), and axial vector (g_A) couplings. The coupling (10) considered above is pseudoscalar, so that our coupling constant $g = g_P$ and the effective potential (11) is due to an exchange of two particles with pseudoscalar couplings. In addition to (11), the exchange of particles with one scalar and one pseudoscalar couplings, as well as with one vector and one axial vector couplings, were considered in [25]. In so doing, in place (10), the Lagrangian density with the scalar coupling is given by

$$\mathcal{L}_S(x) = -g_S \bar{\psi}(x) \psi(x) \varphi(x), \quad (14)$$

whereas the vector field of small mass A_μ is coupled to a fermion field with an interaction of the following form

$$\mathcal{L}_{VA}(x) = \bar{\psi}(x) \gamma^\mu (g_V + g_A \gamma_5) \psi(x) A_\mu(x), \quad (15)$$

where γ^μ with $\mu = 0, 1, 2, 3$ are the Dirac matrices.

Thus, the exchange of particles with one scalar and one pseudoscalar couplings between two similar fermions results in the following effective potential [25]

$$V_{SP}(r) = \frac{g_S^2 g_P^2}{32\pi^2 m r^2} e^{-2r/\lambda}, \quad (16)$$

where λ is the Compton wavelength of a spin-0 particle. The effective potential due to an exchange of particles with one vector and one axial vector couplings is analogous to (16) [25].

Some other spin-independent effective potentials have also been considered in the literature. For example, such kind potentials arise between two fermions due to the massive neutrino-antineutrino exchange where the direct coupling to fermions is effected by the Z bosons [103]. The possibilities of constraining the resulting intermolecular forces by means of molecular spectroscopy are investigated in [104].

5. Constraints on the Spin-Dependent Interactions

As was already mentioned above, the originally introduced axions [6,7] are the pseudo Nambu-Goldstone bosons and their interaction with fermions is described not by the Lagrangian density (10) but by the pseudovector Lagrangian density [88,89]

$$\mathcal{L}_{PV}(x) = \frac{g}{2m_a} \bar{\psi}(x) \gamma_5 \gamma_\mu \psi(x) \partial^\mu \varphi(x). \quad (17)$$

The effective interaction constant in this Lagrangian density $g/(2m_a)$ is not dimensionless and, as a consequence, the respective quantum field theory is nonrenormalizable. On a tree level, however, both Lagrangian densities (10) and (17) result in the same action as can be seen performing the integration by parts. Because of this, both (10) and (17) lead to common spin-dependent effective potential caused by the exchange of one axion between two fermions [18,20,87,105]

$$V(r, \sigma_1, \sigma_2) = \frac{g^2}{16\pi m^2} \left[(\sigma_1 \cdot \mathbf{k})(\sigma_2 \cdot \mathbf{k}) \left(\frac{m_a^2}{r} + 3 \frac{m_a}{r^2} + \frac{3}{r^3} \right) - (\sigma_1 \cdot \sigma_2) \left(\frac{m_a}{r^2} + \frac{1}{r^3} \right) \right] e^{-m_a r}. \quad (18)$$

Here, the same notations, as in Section 4, are used and $\sigma_1/2, \sigma_2/2$ are the fermion spins whereas \mathbf{k} is the unit vector $\mathbf{k} = (\mathbf{r}_1 - \mathbf{r}_2)/r$.

Unfortunately, all experiments of the Casimir physics performed up to date, as well as gravitational experiments, deal with the unpolarized test bodies. As a result, the interaction governed by (18) averages to zero when integrated over their volumes. For this reason, in Section 4 it was necessary to deal with the effective potential (11) which describes the two-axion exchange governed by the Lagrangian density (10). It is interesting that the effective potential of an exchange by the two originally introduces axions, whose interaction with fermions is described by the Lagrangian density (17), is still unknown [25]. Because of this the results of Section 4 are only applicable to the GUT axionlike particles. Below we consider two laboratory experiments which exploit the effective potential (18) and, thus, the constraints obtained from them pertain equally to all types of axions and axionlike particles.

We begin with the comagnetometer experiment [106] adapted for searches the anomalous spin-dependent interaction between the mixture of K and ^3He atoms and the ^3He spin source spaced at a distance of 50 cm. In this experiment, the energy resolution of 10^{-25} eV has been reached [106] giving the possibility to place strong constraints on the interaction potential (18) with the coupling constant of axions to neutrons $g = g_P$. Strong constraints were placed also on the effective potentials [106]

$$V_1(r) = \frac{g_A^2}{4\pi r} (\sigma_1 \cdot \sigma_2) e^{-m_A r} \quad (19)$$

and

$$V_2(r) = -\frac{g_V g_A}{4\pi m} ([\sigma_1 \times \sigma_2] \cdot \mathbf{k}) \left(\frac{m_A}{r} + \frac{1}{r^2} \right) e^{-m_A r}, \quad (20)$$

which are caused by an exchange of light boson A_μ with the mass m_A coupled to fermions by (15).

We illustrate the relative role of magnetometer measurements, on the one hand, and the gravitational experiments and Casimir physics, on the other hand, in constraining the axion-to-nucleon coupling in Figure 4 (recall that the coupling constants of an axion to a proton and a neutron are assumed to be equal). The line marked m in Figure 4 shows the constraints on the coupling constant $g = g_P$ of the effective potential (18) as a function of the axion mass m_a in the logarithmic scale obtained from the comagnetometer measurements [106]. The vertical line 1 at $m_a = 1 \mu\text{eV}$ indicates the current border between the strongest laboratory constraints on the coupling constant of axions to nucleons obtained from

the comagnetometer measurements ($m_a < 1 \mu\text{eV}$) and from the gravitational experiments and Casimir physics ($m_a \geq 1 \mu\text{eV}$). At $m_a \geq 1 \mu\text{eV}$ in Figure 4 we plot the envelope curve of the strongest constraints on the coupling constant of axions to nucleons from the gravitational experiments and Casimir physics shown in Figure 3.

In the region of larger axion masses the constraints on g obtained from the Casimir physics are greatly surpassed by the constraints found from the experiment with a beam of molecular hydrogen [107]. In this experiment, the accurately measured dipole-dipole forces between two protons in the beam of molecular hydrogen have been compared with theory. The constraints on the coupling constant $g = g_P$ in the potential (18) describing an exchange of one axion between two nucleons were obtained from the measure of agreement between experiment and theory. These constraints are shown by the line labeled H_2 in Figure 4. They remain the strongest ones with decreasing axion mass down to $m_a = 0.5 \text{ eV}$. For smaller axion masses the strongest constraints on g follow from the Casimir physics and Cavendish-type experiments. The vertical line 2 in Figure 4 plotted at $m_a = 0.5 \text{ eV}$ separates the constraints on the coupling constant of axions to nucleons obtained from the Casimir physics and from the interaction of protons in a beam of molecular hydrogen. One can conclude that at the moment the gravitational experiments and Casimir physics provide the strongest laboratory constraints on the coupling of axionlike particles to nucleons over the wide range of axion masses from $m_a = 1 \mu\text{eV}$ to 0.5 eV .

Note that the constraints of line H_2 in Figure 4 remain the strongest ones up to $m_a = 200 \text{ eV}$. For larger m_a they are replaced with the stronger constraints found from the comparison between the measurement data of the magnetic resonance experiment and theory for the spin-spin interactions in deuterated molecular hydrogen [108]. Using the same approach, the strongest constraints on the interaction constant g_A of the effective potential (19) were obtained in the region of masses of axial vector bosons $m_A \leq 1000 \text{ eV}$ [108].

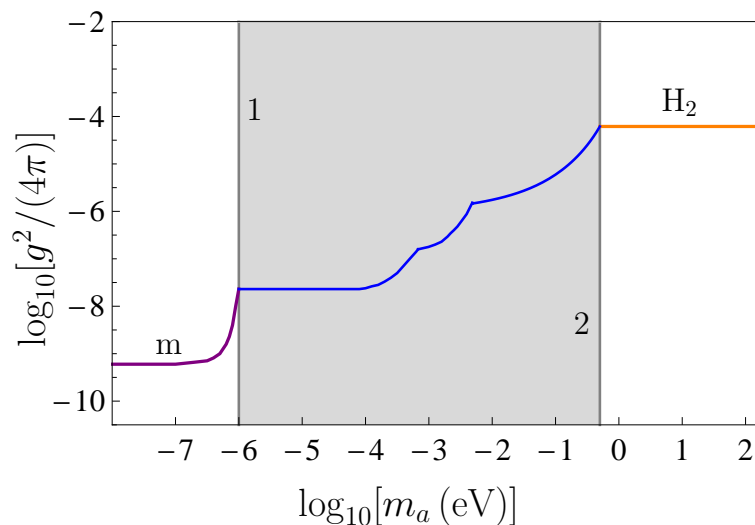


Figure 4. The strongest laboratory constraints on the coupling constant of axions and axionlike particles to nucleons obtained from the magnetometer measurements (line labeled "m") and from the experiment with a beam of molecular hydrogen (line labeled " H_2 "). The vertical lines labeled 1 and 2 indicate the current borders for the strongest constraints obtained from the gravitational experiments and Casimir physics which are shown by the envelope curve in between the lines 1 and 2. The plane areas above the lines are excluded and below them are allowed by the measurement data.

Very recently a Rb-²¹Ne comagnetometer using a SmCo₅ magnet as a spin source was employed to obtain constraints on the products of the pseudoscalar and axial vector electron and neutron couplings to light bosons $g_P^e g_P^n$ and $g_A^e g_A^n$ [109]. In so doing the coupling constants g_P and g_A belong to the spin-dependent effective potentials (18) and (19), respectively, describing an interaction of the pseudoscalar and vector bosons with either an electron or a neutron. As a result, the following constraints have been obtained:

$$g_P^e g_P^n < 1.7 \times 10^{-14}, \quad g_A^e g_A^n < 5 \times 10^{-42}, \quad (21)$$

which is valid for the boson masses below 1 μ eV [109].

Many other laboratory experiments on constraining the hypothetical interactions of different types have been performed which are not directly relevant to the Casimir physics. For instance, a constraint on the coupling constant of electron-electron axial vector interaction $(g_A^e)^2/(4\pi) \leq 4.6 \times 10^{-12}$ arising due to an exchange of spin-1 boson with masses $1 \text{ eV} < m_A < 20 \text{ eV}$ was found in [110] basing on measurements of the magnetic dipole-dipole interaction between two Fe atoms [111,112]. A stronger constraints $(g_A^e)^2/(4\pi) \leq 1.2 \times 10^{-17}$ within another range of boson masses $m_A \leq 0.1 \text{ eV}$ was obtained [113] from measuring the magnetic interaction between two trapped ⁸⁸Sr⁺ ions [114]. The coupling constant g_A of the effective potential (19) describing the electron-muon interaction was constrained [115] for the spin-1 boson masses $m_A \sim 4 \text{ keV}$ by comparing the spectroscopic measurements with precise QED calculations. Much work was also done on constraining the hypothetical interactions which depend on both spins and velocities of the interacting particles (see, e.g., [116,117]).

The experimental tests considered in this section gave the possibility to determine the region of parameters where the constraints obtained from the Casimir physics are the strongest ones. It is possible, however, to constrain the spin-dependent hypothetical interactions directly by measuring the Casimir interaction between two polarized test bodies. In this case the additional interaction caused, e.g., by the effective potential (18) is not averaged to zero after the integration over their volumes and one can obtain the constraints on g and m_a from the measure of agreement between experiment and theory. The Casimir experiments of this kind were proposed in [118]. One option considered in [118] is to use the magnetic test bodies made, for instance, of the ferromagnetic metal Ni (note that the Casimir interaction between two Ni-coated test bodies was already measured in [119,120] but Ni in that experiment was not magnetized). It is significant that at the experimental distances a magnetization of the test bodies results in a spatially homogeneous magnetic force which makes no impact on the measured gradient of the Casimir force. This experiment could lead [118] to the constraints on the coupling constant of axions to electrons which are by several orders of magnitude weaker than those already obtained for solar axions produced by the Compton process and bremsstrahlung [121].

A more prospective possibility suggested in [118] is to constrain the interaction (18) between nucleons by measuring the Casimir interaction for the test bodies possessing the nuclear polarization. It has long been known that spin polarization can be transferred from atomic electrons to nuclei. For the silicon carbide test bodies (this material was already used in measurements of the Casimir force discussed above [59,60]) one can reach the 99% polarization of ²⁹Si nuclear spins in silicon carbide by means of the optical pumping [122]. Calculations show [118] that measurements of the gradient of the Casimir force between the silicon carbide test bodies possessing the nuclear polarization could lead to stronger constraints on the coupling constant of axions to nucleons for the axion masses $m_a \sim 1 \text{ eV}$.

6. Constraints on Some Exotic Particles

Light and massless hypothetical particles considered above and their interactions with particles of the Standard Model are described by the conventional formalism of local quantum field theory and respective effective potentials. As mentioned in Section 1, one of the crucial problems of modern physics

is the problem of dark energy which contributes 68% of the Universe energy and is responsible for the acceleration of the Universe expansion [4]. In an effort to understand the structure of dark energy, several exotic particles have been introduced in the literature whose properties are not unchanged, as for all conventional elementary particles, but depend on the environmental conditions.

The first such particle is the so-called *chameleon* which is described by the real self-interacting scalar field ϕ with a variable mass [13]. This particle becomes heavier, i.e., it has a shorter interaction range, in more dense environments and lighter in the free space. The simplest field equation for the static chameleon field can be written as [13,123]

$$\Delta\phi = \frac{\partial V(\phi)}{\partial\phi} + \frac{\rho}{M} e^{\phi/M}, \quad (22)$$

where $V(\phi)$ is the self-interaction potential, M is the typical mass of the background matter fields, and ρ is the density of background matter. An interaction with the background matter leads to a dependence of the chameleon mass on ϕ [123]

$$m(\phi) = m_0 e^{\phi/M}, \quad (23)$$

where m_0 is the bare mass.

In the region of high matter density, for instance, on the Earth, $m(\phi)$ can be rather large and, thus, the respective interaction sufficiently short-ranged to avoid observable violations of the equivalence principle and the inverse square law of Newtonian gravity. In the region of low matter density, however, e.g., in the cosmic space, some new physics may appear.

There are several chameleon models depending on a specific form of the potential $V(\phi)$ [123]. For us it is important that an exchange of chameleons between two test bodies leads to some additional force between them which can be constrained in experiments on measuring the Casimir force. The character of this force depends on both the chameleon model and on the experimental configuration. In the configuration of two parallel plates and a sphere above a plate the additional chameleon force was calculated in [123], and some constraints on it following from the already performed experiments were found for different types of the chameleon potential. In [124] the new experiment was proposed on measuring the Casimir force between two parallel plates at large separations exceeding $10\ \mu\text{m}$. This allows to test different chameleon models by varying the density of matter in a gap between the plates. The proposed experiment was further elaborated and developed in [84,85,125,126]. Its realization is of much promise for this field.

The other kinds of exotic particles suggested in order to explain the nature of dark energy are *symmetrons*. These particles are described by the self-interacting real scalar field whose interaction constant with matter depends on the density of an environment [14,127,128]. Symmetrons interact with matter weaker if the environment density is higher. Similar to chameleons, this property helps them to escape notice in gravitational experiments of Eötvös and Cavendish type. In the static case the symmetron field satisfies the equation [14,127]

$$\Delta\phi = \frac{\partial V(\phi)}{\partial\phi} + \left(\frac{\rho}{M^2} - \mu^2 \right) \phi, \quad (24)$$

where μ is the symmetron mass and all other notations are the same as in (22).

Similar to the case of chameleons, there should be some additional force which arises between two closely spaced test bodies due to the exchange of symmetrons. Because of this, measurements of the Casimir interaction can be used for constraining the parameters of symmetron models. The forces arising due to an exchange of symmetrons between two dense parallel plates separated by a vacuum gap, as well

as between a sphere and a plate, were found in [129]. The experiment using the sphere-plate geometry was proposed which is capable to place strong constraints on the models of symmetron in near future [129]. In addition to the chameleons and symmetrons, the properties of some other exotic particles, e.g., the dilaton introduced in string theory, depend on the environment [130].

Explanation of the accelerated expansion of the Universe in the framework of Einstein's general relativity theory requires the stress-energy tensor describing the negative pressure of some material medium. Besides the chameleon and symmetron fields, this property is offered by the stress-energy tensor of the Maxwell-Proca electrodynamics in the case of nonzero photon mass [131]. An impact of the negative pressure originating from the Maxwell stress-energy tensor of massive photons on the interstellar gas, on stars in the process of their formation and on the rotational dynamics of galaxies was investigated.

The effect of a nonzero photon mass on the Casimir-Polder interaction between two polarized particles was considered in [132] with applications to several theoretical approaches beyond the Standard Model. It was noted that the absence of deviations in the standard Casimir-Polder force calculated using the massless photons from the measurement data could be used to place new constraints on some extradimensional models.

The constraints on the so-called *hidden photons*, i.e., light spin-1 bosons, which are predicted in the framework of string theory and do not interact directly with elementary particles of the Standard Model, are obtained in [133] from experiments on measuring the Casimir force and testing the Coulomb law. Further improvement of these constraints is expected in future with increasing precision of relevant measurements.

7. Implications for the Quantum Vacuum, Dark Energy, and the Cosmological Constant

One of the major unresolved problems of the Standard Model is the problem of energy of the quantum vacuum. It is usually believed that the standard quantum field theory should be applicable at all energies below the Planck energy $E_{\text{Pl}} = 1/\sqrt{G} \sim 10^{19} \text{ GeV} \sim 10^9 \text{ J}$. The vacuum energy density of quantum fields is given by the divergent intergrals with respect to momentum

$$\varepsilon_{\text{vac}} = \frac{1}{2(2\pi)^2} \int d^3p \left(\sum_{l=1}^H h_l \sqrt{m_l^2 + p^2} - \sum_{l=1}^F f_l \sqrt{M_l^2 + p^2} \right). \quad (25)$$

Here, H bosonic fields with masses m_l and degrees of freedom h_l and F fermionic fields with masses M_l and degrees of freedom f_l contribute to the result. When making a cutoff at the Planck momentum $p_{\text{Pl}} = E_{\text{Pl}}/c$, we obtain the huge energy density $\varepsilon_{\text{vac}} \sim 10^{11} \text{ J/m}^3$. However, the vacuum energy density needed to explain the observed acceleration of the Universe expansion is of the order of $\varepsilon_{\text{vac}}^{\text{obs}} = 10^{-9} \text{ J/m}^3$ which is different from the above value by the factor of 10^{120} [134,135]. Considering that the vacuum energy density can be interpreted in terms of the cosmological constant Λ in Einstein's equations [136], so huge difference between its predicted and observed values is sometimes called *the vacuum catastrophe* [2].

In fact a consideration of the exotic particles and fields in Section 6, such as chameleons, symmetrons, massive photons, etc., aims to explain the nature of a background medium possessing the energy density of about 10^{-9} J/m^3 and contributing approximately 68% to the total energy of the Universe. To ensure the observed acceleration of the Universe expansion, this medium should possess the negative pressure $p_{\text{vac}}^{\text{obs}} = -\varepsilon_{\text{vac}}^{\text{obs}} < 0$. This property is guarantied by the cosmological term in Einstein's equations

$$R_{ik} - \frac{1}{2} R g_{ik} + \Lambda g_{ik} = -8\pi G T_{ik}, \quad (26)$$

where R_{ik} , g_{ik} , and T_{ik} are the Ricci, metrical, and stress-energy tensors. The cosmological constant in (26) is connected with the observed vacuum energy density according to

$$\Lambda = 8\pi G\varepsilon_{\text{vac}}^{\text{obs}} \approx 2 \times 10^{-52} \text{ m}^{-2}. \quad (27)$$

Taking into account that both the Casimir force and the cosmological constant may have joint origin in the zero-point oscillations of the quantum vacuum, the question arises about the possibility of their common theoretical description. The point is that the Casimir effect is well understood in the framework of the Lifshitz theory [137,138]. In doing so the finite Casimir energy density is obtained as a difference between two infinite quantities calculated in the presence of a material medium with appropriate boundary conditions and in the free space. The respective force was measured in numerous experiments and found to be in agreement with theory [47,48].

Recently an attempt was undertaken to develop the Lifshitz-type theory of the cosmological constant [139]. This attempt is based on an observation that the space-time geometry can be treated as an effective medium for the electromagnetic field. The medium under consideration is characterized by some index of refraction n and the expansion of space is described as the time dependence of $n = n(t)$. According to the argumentation of [139], the expanding flat space is indistinguishable from the uniform medium having the refraction index depending on time. Under an assumption of similar response to the electric and magnetic fields, $\varepsilon = \mu$ and, thus, $n = \sqrt{\varepsilon\mu} = \varepsilon$, the contribution of the electromagnetic field to the cosmological constant was found. This approach, however, does not predict some specific value of Λ because it is considered not as a constant but as a dynamic quantity [139]. A comparison of the developed theoretical scheme with the experimental data remains to be made.

Another approach considers the cosmological constant as one of the fundamental constants of nature. Within this approach, it is not a problem that the bare value of the cosmological constant $\Lambda_b = 8\pi G\varepsilon_{\text{vac}}$ is infinitely large. It is only important that its renormalized value is given by (27). From this point of view only the quantity $\varepsilon_{\text{vac}}^{\text{obs}}$ represents the source of the gravitational field whereas the infinitely large ε_{vac} , representing the energy density of virtual particles, does not gravitate [140,141]. Although this approach could be finally approved only in the framework of missing quantum gravity, it seems to be in close analogy with the Casimir effect where only a difference between two infinite sets of the zero-point oscillations, with and without the material boundaries, contributes to the observable energy density and force.

In any case, the tests of dark energy by means of atomic interferometry and neutron scattering [142, 143] along with that ones considered above by means of the Casimir and gravitational experiments should shed more light on this puzzling form of matter.

8. Discussion

In the foregoing, we have considered different theoretical predictions beyond the Standard Model and constraints on them following from measurements of the Casimir force and several other laboratory experiments which cover the parameter regions neighboring to those covered by the Casimir effect. It turns out that the predicted interactions and elementary particles lead to a wide variety of effective potentials and respective forces which could act between the test bodies in addition to familiar fundamental interactions of the Standard Model. During the last decades, a lot of experiments have been performed attempting to discover these forces or at least to constrain their parameters. Here, we restricted our consideration to the constraints obtained from measuring the Casimir force supplemented with the gravitational experiments, neutron scattering, magnetometer measurements etc.

One of the most interesting subjects is the possibility of new power-type interactions decreasing with separation faster than the gravitational and electric ones. The constraints on the potentials of the form

r^{-n} with $n > 1$ were obtained from the Cavendish-type experiments and remained unchanged for more than a decade. The progress in obtaining the stronger constraints reflected in Section 2 has been made only in 2020 for the potentials with $n = 2, 3, 4$, and 5 by using the measurement results of the further improved Cavendish-type experiment. It seems that additional strengthening of the obtained constraints may require new experimental approaches.

The potentials and forces of Yukawa-type are of no less importance. They are predicted in many theoretical schemes beyond the Standard Model and were tested in numerical experiments. Measurements of the Casimir force are the recognized source of constraints on the Yukawa-type potentials but there is a permanent competition between different tests on whether or not this particular test leads to the strongest constraints within some specific interaction range. In Section 3, we have reflected the present situation in this subject. Unlike the case of power-type potentials, here the state of affairs changes rapidly and new important results might be expected in near future.

The spin-independent potentials different from the Yukawa one were considered in Section 4. The most important of them describes an exchange of two axionlike particles between two fermions. The constraints on the coupling constant and mass of axionlike particles were obtained by using this process from the Casimir effect and gravitational experiments. These constraints compete between themselves and with the constraints of another type which are obtained from the experiments sensitive to an exchange of one axion. The more exotic spin-independent potentials discussed by us may become more usable in the coming years.

The exchange of one axion between two fermions is described by the spin-dependent potential which is used for constraining both the originally introduced axions and axionlike particles by means of the magnetometer measurements, measurements of dipole-dipole forces between two protons in the beams of molecular hydrogen and in some other laboratory experiments. These experiments are complementary to the Casimir physics and gravitational measurements in constraining the axion-nucleon interaction on a laboratory table. The constraints on several more exotic spin-dependent potentials under discussion in the literature were also considered in Section 5. There are many suggestions of this kind and their detailed consideration is beyond the scope of the present review where we discussed only a few typical examples.

The hypothetical constituents of dark energy, such as chameleons, symmetrons, massive photons etc., as well as the constraints on them from different laboratory experiments including measurements of the Casimir force, were discussed in Section 6. The main problem here is somewhat indefinite character of the theoretical predictions which admit distinct forms of potentials and different values of the involved parameters. The diverged approaches to a description of the dark energy and the cosmological constant considered in Section 7 demonstrate that we are still far from understanding of their physical nature.

9. Conclusions

To conclude, the Casimir effect allows to place strong constraints on many theoretical predictions beyond the Standard Model including the spin-independent and spin-dependent interactions and exotic particles and fields introduced for an understanding of the nature of dark energy. The borders of parameter regions, where the Casimir effect leads to the strongest constraints, are determined from some other laboratory experiments. In near future one could expect that more important results will be obtained using new generation of experiments in the configuration of parallel plates spaced at separations about $10 \mu\text{m}$ and differential force measurements with sensitivity below a femtonewton. Because of this, it is very probable that testing and constraining the far-reaching predictions of the supersymmetry, supergravity, string theory and other sophisticated theoretical approaches will be made not only with the more powerful accelerators of next generations, but with precision tabletop laboratory experiments.

Funding: This work was supported by the Peter the Great Saint Petersburg Polytechnic University in the framework of the Russian state assignment for basic research (project N FSEG-2020-0024).

Acknowledgments: The author is grateful to H. Abele, A.A. Banishev, V.B. Bezerra, M. Bordag, R. Castillo-Garza, C.-C. Chang, H.C. Chiu, R.S. Decca, E. Fischbach, D.E. Krause, P. Kuusk, D. López, V.N. Marachevsky, U. Mohideen, V.M. Mostepanenko, C. Romero, and R.I.P. Sedmik for collaboration in our joint publications used in this review.

Conflicts of Interest: The author declares no conflict of interest.

References

1. Rovelli, C. *Quantum Gravity*; Cambridge University Press: Cambridge, UK, 2004.
2. Adler, R.J.; Casey, B.; Jacob, O.C. Vacuum catastrophe: An elementary exposition of the cosmological constant problem. *Amer. J. Phys.* **1995**, *63*, 620–626.
3. Peccei, R.D. The Strong CP Problem and Axions. *Lect. Notes Phys.* **2008**, *741*, 3–17.
4. Matarrese, S.; Colpi, M.; Gorini, V.; Moshella, U. (Eds.) *Dark Matter and Dark Energy*; Springer: Dordrecht, Netherlands, 2011.
5. Anselm, A.A.; Uraltsev, N.G. A second massless axion? *Phys. Lett. B* **1982**, *114*, 39–41.
6. Weinberg, S. A New Light Boson? *Phys. Rev. Lett.* **1978**, *40*, 223–226.
7. Wilczek, F. Problem of Strong P and T Invariance in the Presence of Instantons. *Phys. Rev. Lett.* **1978**, *40*, 279–283.
8. Peccei, R.D.; Quinn, H.R. CP Conservation in the Presence of Pseudoparticles. *Phys. Rev. Lett.* **1977**, *38*, 1440–1443.
9. Ferrara, S.; Scherk, J.; Zumino, B. Algebraic properties of extended supergravity theories. *Nucl. Phys. B* **1977**, *121*, 393–402.
10. Fujii, Y. The theoretical background of the fifth force. *Int. J. Mod. Phys. A* **1991**, *6*, 3505–3557.
11. Salam, A.; Strathdee, J. On goldstone fermions. *Phys. Lett. B* **1974**, *49*, 465–467.
12. Deser, S.; Zumino, B. Broken Supersymmetry and Supergravity. *Phys. Rev. Lett.* **1977**, *38*, 1433–1436.
13. Khoury, J.; Weltman, A. Chameleon cosmology. *Phys. Rev. D* **2004**, *69*, 044026.
14. Olive, K.A.; Pospelov, M. Environmental dependence of masses and coupling constants. *Phys. Rev. D* **2008**, *77*, 043524.
15. Fischbach, E.; Talmadge, C.L. *The Search for Non-Newtonian Gravity*; Springer-Verlag: New York, USA, 1999.
16. Randall, L.; Sundrum, R. Large Mass Hierarchy from a Small Extra Dimension. *Phys. Rev. Lett.* **1999**, *83*, 3370–3373.
17. Randall, L.; Sundrum, R. An Alternative to Compactification. *Phys. Rev. Lett.* **1999**, *83*, 4690–4693.
18. Bohr, A.; Mottelson, B.R. *Nuclear Structure, Vol. 1*; Benjamin: New York, USA, 1969.
19. Ferrer, F.; Nowakowski, M. Higg- and Goldstone-boson-mediated long range forces. *Phys. Rev. D* **1999**, *59*, 075009.
20. Adelberger, E.G.; Fischbach, E.; Krause, D.E.; Newman, R.D. Constraining the couplings of massive pseudoscalars using gravity and optical experiments. *Phys. Rev. D* **2003**, *68*, 062002.
21. Antoniadis, I.; Arkani-Hamed, N.; Dimopoulos, S.; Dvali, G. New dimensions at a millimeter to a fermi and superstrings at a TeV. *Phys. Lett. B* **1998**, *436*, 257–263.
22. Arkani-Hamed, N.; Dimopoulos, S.; Dvali, G. Phenomenology, astrophysics, and cosmology of theories with millimeter dimensions and TeV scale quantum gravity. *Phys. Rev. D* **1999**, *59*, 086004.
23. Floratos, E.G.; Leontaris, G.K. Low scale unification, Newton’s law and extra dimensions. *Phys. Lett. B* **1999**, *465*, 95–100.
24. Kehagias, A.; Sfetsos, K. Deviations from $1/r^2$ Newton law due to extra dimensions. *Phys. Lett. B* **2000**, *472*, 39–44.
25. Aldaihan, S.; Krause, D.E.; Long, J.C.; Snow, W.M. Calculations of the dominant long-range, spin-independent contributions to the interaction energy between two nonrelativistic Dirac fermions from double-boson exchange of spin-0 and spin-1 bosons with spin-dependent couplings. *Phys. Rev. D* **2017**, *95*, 096005.

26. Adelberger, E.G.; Heckel, B.R.; Stubbs, C.W.; Rogers, W.F. Searches for new Macroscopic forces. *Annu. Rev. Nucl. Part. Sci.* **1991**, *41*, 269–320.
27. Rosenberg, L.J.; van Bibber, K.A. Searches for invisible axions. *Phys. Rep.* **2000**, *325*, 1–39.
28. Antoniadis, I.; Baessler, S.; Bücher, M.; Fedorov, V. V.; Hoedl, S.; Lambrecht, A.; Nesvizhevsky, V. V.; Pignol, G.; Protasov, K. V.; Reynaud, S.; Sobolev, Yu. Short-range fundamental forces. *Compt. Rend.* **2011**, *12*, 755–778.
29. Ivastorza, I.G.; Redondo, J. New experimental approaches in the search for axion-like particles. *Progr. Part. Nucl. Phys.* **2018**, *102*, 89–159.
30. Safronova, M.S.; Budker, D.; DeMille, D.; Jackson Kimball, D.F.; Derevianko, A.; Clark, C.W. Search for new physics with atoms and molecules. *Rev. Mod. Phys.* **2018**, *90*, 025008.
31. Kuzmin, V.A.; Tkachev, I.I.; Shaposhnikov, M.E. Restrictions imposed on light scalar particles by measurements of van der Waals forces. *Pis'ma v Zh. Eksp. Teor. Fiz.* **1982**, *36*, 49–52; Translated: *JETP Lett.* **1982**, *36*, 59–62.
32. Blasone, M.; Lambiase, G.; Luciano, G.G.; Petruzzello, L.; Scardigli, F. Heuristic derivation of the Casimir effect in minimal length theories. *Int. J. Mod. Phys. D* **2020**, *29*, 2050011.
33. Blasone, M.; Lambiase, G.; Petruzzello, L.; Stabile, A. Casimir effect in Post-Newtonian gravity with Lorentz-violation. *Eur. Phys. J. C* **2018**, *78*, 976.
34. Mostepanenko, V.M.; Sokolov, I.Yu. Restrictions on long-range forces following from the Casimir effect. *Yadern. Fiz.* **1987**, *46*, 1174–1180; Translated: *Sov. J. Nucl. Phys.* **1987**, *46*, 685–688.
35. Feinberg, G.; Sucher, J. Long-Range Forces from Neutrino-Pair Exchange. *Phys. Rev.* **1968**, *166*, 1638–1644.
36. Fischbach, E. Long-range forces and neutrino mass. *Ann. Phys. (N.Y.)* **1996**, *247*, 213–291.
37. Gundlach, J.H.; Smith, G.L.; Adelberger, E.G.; Heckel, B.R.; Swanson, H.E. Short-Range Test of the Equivalence Principle. *Phys. Rev. Lett.* **1997**, *78*, 2523–2526.
38. Smith, G.L.; Hoyle, C.D.; Gundlach, J.H.; Adelberger, E.G.; Heckel, B.R.; Swanson, H.E. Short-range tests of the equivalence principle. *Phys. Rev. D* **2000**, *61*, 022001.
39. Adelberger, E.G.; Heckel, B.R.; Hoedl, S.; Hoyle, C.D.; Kapner, D.J.; Upadhye, A. Particle-Physics Implications of a Recent Test of the Gravitational Inverse-Square Law. *Phys. Rev. Lett.* **2007**, *98*, 131104.
40. Mostepanenko, V.M.; Sokolov, I.Yu. The Casimir effect leads to new restrictions on long-range force constants. *Phys. Lett. A* **1987**, *125*, 405–408.
41. Derjaguin, B.V.; Abrikosova, I.I.; Lifshitz, E.M. Direct measurement of molecular attraction between solids separated by a narrow gap. *Quat. Rev.* **1956**, *10*, 295–329.
42. Mostepanenko, V.M.; Sokolov, I.Yu. Stronger restrictions on the constants of long-range forces decreasing as r^{-n} . *Phys. Lett. A* **1990**, *146*, 373–374.
43. Fischbach, E.; Krause, D.E. Constraints on Light Pseudoscalars Implied by Tests of the Gravitational Inverse-Square Law. *Phys. Rev. Lett.* **1999**, *83*, 3593–3597.
44. Tan, W.-H.; Du, A.-B.; Dong, W.-C.; Yang, S.-Q.; Shao, C.-G.; Guan, S.-G.; Wang, Q.-L.; Zhan, B.-F.; Luo, P.-S.; Tu, L.-C.; Luo, J. Improvement for Testing the Gravitational Inverse-Square Law at the Submillimeter Range. *Phys. Rev. Lett.* **2020**, *124*, 051301.
45. Liu, J.; Zhu, K.-D. Detecting large extra dimensions with optomechanical levitated sensors. *Eur. Phys. J. C* **2019**, *79*, 18.
46. Brax, P.; Fichet, S.; Pignol, G. Bounding quantum dark forces. *Phys. Rev. D* **2018**, *97*, 115034.
47. Bordag, M.; Klimchitskaya, G.L.; Mohideen, U.; Mostepanenko, V.M. *Advances in the Casimir Effect*; Oxford University Press: Oxford, UK, 2015.
48. Klimchitskaya, G.L.; Mohideen, U.; Mostepanenko, V.M. The Casimir force between real materials: Experiment and theory. *Rev. Mod. Phys.* **2009**, *81*, 1827–1885.
49. Tabor, D.; Winterton, R.H.S. Surface Forces: Direct Measurement of Normal and Retarded van der Waals Forces. *Nature* **1968**, *219*, 1120–1121.
50. Mostepanenko, V.M.; Novello, M. Constraints on non-Newtonian gravity from the Casimir force measurements between two crossed cylinders. *Phys. Rev. D* **2001**, *63*, 115003.
51. Ederth, T. Template-stripped gold surfaces with 0.4-nm rms roughness suitable for force measurements: Application to the Casimir force in the 20–100-nm range. *Phys. Rev. A* **2000**, *62*, 062104.

52. Bezerra, V.B.; Klimchitskaya, G.L.; Mostepanenko, V.M.; Romero, C. Advance and prospects in constraining the Yukawa-type corrections to Newtonian gravity from the Casimir effect. *Phys. Rev. D* **2010**, *81*, 055003.
53. Klimchitskaya, G.L.; Mohideen, U.; Mostepanenko, V.M. Constraints on corrections to Newtonian gravity from two recent measurements of the Casimir interaction between metallic surfaces. *Phys. Rev. D* **2013**, *87*, 125031.
54. Klimchitskaya, G.L.; Kuusk, P.; Mostepanenko, V.M. Constraints on non-Newtonian gravity and axionlike particles from measuring the Casimir force in nanometer separation range. *Phys. Rev. D* **2020**, *101*, 056013.
55. Chiu, H.C.; Klimchitskaya, G.L.; Marachevsky, V.N.; Mostepanenko, V.M.; Mohideen, U. Demonstration of the asymmetric lateral Casimir force between corrugated surfaces in the nonadditive regime. *Phys. Rev. B* **2009**, *80*, 121402(R).
56. Chiu, H.C.; Klimchitskaya, G.L.; Marachevsky, V.N.; Mostepanenko, V.M.; Mohideen, U. Lateral Casimir force between sinusoidally corrugated surfaces: Asymmetric profiles, deviations from the proximity force approximation, and comparison with exact theory. *Phys. Rev. B* **2010**, *81*, 115417.
57. Banishev, A.A.; Wagner, J.; Emig, T.; Zandi, R.; Mohideen, U. Demonstration of Angle-Dependent Casimir Force between Corrugations. *Phys. Rev. Lett.* **2013**, *110*, 250403.
58. Banishev, A.A.; Wagner, J.; Emig, T.; Zandi, R.; Mohideen, U. Experimental and theoretical investigation of the angular dependence of the Casimir force between sinusoidally corrugated surfaces. *Phys. Rev. B* **2014**, *89*, 235436.
59. Sedighi, M.; Svetovoy, V.B.; Broer, W.H.; Palasantzas, G. Casimir forces from conductive silicon carbide surfaces. *Phys. Rev. B* **2014**, *89*, 195440.
60. Sedighi, M.; Svetovoy, V.B.; Palasantzas, G. Casimir force measurements from silicon carbide surfaces. *Phys. Rev. B* **2016**, *93*, 085434.
61. Decca, R.S.; Fischbach, E.; Klimchitskaya, G.L.; Krause, D.E.; López, D.; Mostepanenko, V.M. Improved tests of extra-dimensional physics and thermal quantum field theory from new Casimir force measurements. *Phys. Rev. D* **2003**, *68*, 116003.
62. Decca, R.S.; López, D.; Fischbach, E.; Klimchitskaya, G.L.; Krause, D.E.; Mostepanenko, V.M. Precise comparison of theory and new experiment for the Casimir force leads to stronger constraints on thermal quantum effects and long-range interactions. *Ann. Phys. (N.Y.)* **2005**, *318*, 37–80.
63. Decca, R.S.; López, D.; Fischbach, E.; Klimchitskaya, G.L.; Krause, D.E.; Mostepanenko, V.M. Tests of new physics from precise measurements of the Casimir pressure between two gold-coated plates. *Phys. Rev. D* **2007**, *75*, 077101.
64. Decca, R.S.; López, D.; Fischbach, E.; Klimchitskaya, G.L.; Krause, D.E.; Mostepanenko, V.M. Novel constraints on light elementary particles and extra-dimensional physics from the Casimir effect. *Eur. Phys. J. C* **2007**, *51*, 963–975.
65. Klimchitskaya, G.L.; Mostepanenko, V.M. Constraints on axionlike particles and non-Newtonian gravity from measuring the difference of Casimir forces. *Phys. Rev. D* **2017**, *95*, 123013.
66. Bimonte, G.; López, D.; Decca, R.S. Isoelectronic determination of the thermal Casimir force. *Phys. Rev. B* **2016**, *93*, 184434.
67. Decca, R.S.; López, D.; Chan, H.B.; Fischbach, E.; Krause, D.E.; Jamell, C.R. Constraining New Forces in the Casimir Regime Using the Isoelectronic Technique. *Phys. Rev. Lett.* **2005**, *94*, 240401.
68. Chen, Y.J.; Tham, W.K.; Krause, D.E.; López, D.; Fischbach, E.; Decca, R.S. Stronger Limits on Hypothetical Yukawa Interactions in the 30–8000 Nm Range. *Phys. Rev. Lett.* **2016**, *116*, 221102.
69. Masuda, M.; Sasaki, M. Limits on Nonstandard Forces in the Submicrometer Range. *Phys. Rev. Lett.* **2009**, *102*, 171101.
70. Wang, J.; Guan, S.; Chen, K.; Wu, W.; Tian, Z.; Luo, P.; Jin, A.; Yang, S.; Shao, C.; Luo, J. Test of non-Newtonian gravitational forces at micrometer range with two-dimensional force mapping. *Phys. Rev. D* **2016**, *94*, 122005.
71. Mostepanenko, V.M.; Klimchitskaya, G.L. The State of the Art in Constraining Axion-to-Nucleon Coupling and Non-Newtonian Gravity from Laboratory Experiments. *Universe* **2020**, *6*, 147.
72. Smullin, S.J.; Geraci, A.A.; Weld, D.M.; Chiaverini, J.; Holmes, S.; Kapitulnik, A. Constraints on Yukawa-type deviations from Newtonian gravity at 20 microns. *Phys. Rev. D* **2005**, *72*, 122001.

73. Kapner, D.J.; Cook, T.S.; Adelberger, E.G.; Gundlach, J.H.; Heckel, B.R.; Hoyle, C.D.; Swanson, H.E. Tests of the Gravitational Inverse-Square Law below the Dark-Energy Length Scale. *Phys. Rev. Lett.* **2007**, *98*, 021101.
74. Hoskins, J.K.; Newman, R.D.; Spero, R.; Schultz, J. Experimental tests of the gravitational inverse-square law for mass separations from 2 to 105 cm. *Phys. Rev. D* **1985**, *32*, 3084–3095.
75. Schlamminger, S.; Choi, K.-J.; Wagner, T.A.; Gundlach, J.H.; Adelberger, E.G. Test of the Equivalence Principle Using a Rotating Torsion Balance. *Phys. Rev. Lett.* **2008**, *100*, 041101.
76. Karshenboim, S.G. Constraints on a long-range spin-independent interaction from precision atomic physics. *Phys. Rev. D* **2010**, *82*, 073003.
77. Nesvizhevsky, V.V.; Pignol, G.; Protasov, K.V. Neutron scattering and extra short range interactions. *Phys. Rev. D* **2008**, *77*, 034020.
78. Kamiya, Y.; Itagami, K.; Tani, M.; Kim, G.N.; Komamiya, S. Constraints on New Gravitylike Forces in the Nanometer Range. *Phys. Rev. Lett.* **2015**, *114*, 161101.
79. Haddock, C.C.; Oi, N.; Hirota, K.; Ino, T.; Kitaguchi, M.; Matsumoto, S.; Mishima, K.; Shima, T.; Shimizu, H.M.; Snow, W.M.; Yoshioka, T. Search for deviations from the inverse square law of gravity at nm range using a pulsed neutron beam. *Phys. Rev. D* **2018**, *97*, 062002.
80. Klimchitskaya, G.L. Recent breakthrough and outlook in constraining the non-Newtonian gravity and axion-like particles from Casimir physics. *Eur. Phys. J. C* **2017**, *77*, 315.
81. Hebestreit, E.; Frimmer, M.; Reimann, R.; Novotny, L. Sensing Static Forces with Free-Falling Nanoparticles. *Phys. Rev. Lett.* **2018**, *121*, 063602.
82. Borkowski, M.; Buchachenko, A.A.; Ciuryło, R.; Julianne, P.S.; Yamada, H.; Kikuchi, Y.; Takasu, Y.; Takahashi, Y. Weakly bound molecules as sensors of new gravitylike forces. *Sci. Rep.* **2019**, *9*, 14807.
83. Bennett, R.; O'Dell, D.H.J. Revealing short-range non-Newtonian gravity through Casimir-Polder shielding. *New J. Phys.* **2019**, *21*, 033032.
84. Sedmik, R.; Brax, P. Status Report and first Light from Cannex: Casimir Force Measurements between flat parallel Plates. *J. Phys.: Conf. Ser.* **2018**, *1138*, 012014.
85. Klimchitskaya, G.L.; Mostepanenko, V.M.; Sedmik, R.I.P.; Abele, H. Prospects for Searching Thermal Effects, Non-Newtonian Gravity and Axion-Like Particles: CANNEX Test of the Quantum Vacuum. *Symmetry* **2019**, *11*, 407.
86. Yang, S.-H.; Pi, C.-M.; Zheng, X.-P.; Weber, F. Non-Newtonian Gravity in Strange Quark Stars and Constraints from the Observations of PSR J0740+6620 and GW170817. *ApJ* **2020**, *902*, 32.
87. Moody, J.E.; Wilczek, F. New macroscopic forces? *Phys. Rev. D* **1984**, *30*, 130–139.
88. Kim, J.E. Light pseudoscalars, particle physics and cosmology. *Phys. Rep.* **1987**, *150*, 1–177.
89. Raffelt, G.G. Axions – motivation, limits and searches. *J. Phys. A: Math. Theor.* **2007**, *40*, 6607–6620.
90. Drell, S.D.; Huang, K. Many-Body Forces and Nuclear Saturation. *Phys. Rev.* **1953**, *91*, 1527–1543.
91. Raffelt, G. Limits on a CP-violating scalar axion-nucleon interaction. *Phys. Rev. D* **2012**, *86*, 015001.
92. Bezerra, V.B.; Klimchitskaya, G.L.; Mostepanenko, V.M.; Romero, C. Constraints on the parameters of an axion from measurements of the thermal Casimir-Polder force. *Phys. Rev. D* **2014**, *89*, 035010.
93. Obrecht, J.M.; Wild, R.J.; Antezza, M.; Pitaevskii, L.P.; Stringari, S.; Cornell, E.A. Measurement of the Temperature Dependence of the Casimir-Polder Force. *Phys. Rev. Lett.* **2007**, *98*, 063201.
94. Bezerra, V.B.; Klimchitskaya, G.L.; Mostepanenko, V.M.; Romero, C. Stronger constraints on an axion from measuring the Casimir interaction by means of a dynamic atomic force microscope. *Phys. Rev. D* **2014**, *89*, 075002.
95. Chang, C.C.; Banishev, A.A.; Castillo-Garza, R.; Klimchitskaya, G.L.; Mostepanenko, V.M.; Mohideen, U. Gradient of the Casimir force between Au surfaces of a sphere and a plate measured using an atomic force microscope in a frequency-shift technique. *Phys. Rev. B* **2012**, *85*, 165443.
96. Bezerra, V.B.; Klimchitskaya, G.L.; Mostepanenko, V.M.; Romero, C. Constraining axion-nucleon coupling constants from measurements of effective Casimir pressure by means of micromachined oscillator. *Eur. Phys. J. C* **2014**, *74*, 2859.

97. Bezerra, V.B.; Klimchitskaya, G.L.; Mostepanenko, V.M.; Romero, C. Constraints on axion-nucleon coupling constants from measuring the Casimir force between corrugated surfaces. *Phys. Rev. D* **2014**, *90*, 055013.
98. Klimchitskaya, G.L.; Mostepanenko, V.M. Improved constraints on the coupling constants of axion-like particles to nucleons from recent Casimir-less experiment. *Eur. Phys. J. C* **2015**, *75*, 164.
99. Spero, R.; Hoskins, J.K.; Newman, R.; Pellam, J.; Schultz, J. Test of the Gravitational Inverse-Square Law at Laboratory Distances. *Phys. Rev. Lett.* **1980**, *44*, 1645–1648.
100. Long, J.C.; Chan, H.W.; Churnside, A.B.; Gulbis, E.A.; Varney, M.C.M.; Price, J.C. Upper limits to submillimetre-range forces from extra space-time dimensions. *Nature* **2003**, *421*, 922–925.
101. Yan, H.; Housworth, E.A.; Meyer, H.O.; Visser, G.; Weisman, E.; Long, J.C. Absolute measurement of thermal noise in a resonant short-range force experiment. *Class. Quant. Grav.* **2014**, *31*, 205007.
102. Long, J.C.; Kostelecký, V.A. Search for Lorentz violation in short-range gravity. *Phys. Rev. D* **2015**, *91*, 092003.
103. Grifols, J.A.; Massó, E.; Toldrà, R. Majorana neutrinos and long range forces. *Phys. Lett. B* **1996**, *389*, 563–565.
104. Hollik, W.G.; Linster, M.; Tabet, T. A study of New Physics searches with tritium and similar molecules. *Eur. Phys. J. C* **2020**, *80*, 661.
105. Daido, R.; Takahashi, F. The sign of the dipole-dipole potential by axion exchange, *Phys. Lett. B* **2017**, *772*, 127–129.
106. Vasilakis, G.; Brown, J.M.; Kornak, T.R.; Romalis, M.V. Limits on New Long Range Nuclear Spin-Dependent Forces Set with a $K\text{-}^3\text{He}$ Comagnetometer. *Phys. Rev. Lett.* **2009**, *103*, 261801.
107. Ramsey, N.F. The tensor force between two protons at long range. *Physica A* **1979**, *96*, 285–289.
108. Ledbetter, M.P.; Romalis, M.V.; Jackson Kimball, D.F. Constraints on Short-Range Spin-Dependent Interactions from Scalar Spin-Spin Coupling in Deuterated Molecular Hydrogen. *Phys. Rev. Lett.* **2013**, *110*, 040402.
109. Almasi, A.; Lee, J.; Winarto, H.; Smiciklas, M.; Romalis, M.V. New Limits on Anomalous Spin-Spin Interactions. *Phys. Rev. Lett.* **2020**, *125*, 201802.
110. Luo, P.; Ding, J.; Wang, J.; Ren, X. Constraints on spin-dependent exotic interactions between electrons at the nanometer scale. *Phys. Rev. D* **2017**, *96*, 055028.
111. Choi, T.; Paul, W.; Rolf-Pissarczyk, S.; Macdonald, A.J.; Natterer, F.D.; Yang, K.; Willke, P.; Lutz, C.P.; Heinrich, A.J. Atomic-scale sensing of the magnetic dipolar field from single atoms. *Nature Nanotech.* **2017**, *12*, 420.
112. Baumann, S.; Paul, W.; Choi, T.; Lutz, C.P.; Ardavan, A.; Heinrich, A.J. Electron paramagnetic resonance of individual atoms on a surface. *Science* **2015**, *350*, 417.
113. Kotler, S.; Ozeri, R.; Jackson Kimball D.F. Constraints on Exotic Dipole-Dipole Couplings between Electrons at the Micrometer Scale. *Phys. Rev. Lett.* **2015**, *115*, 081801.
114. Kotler, S.; Akerman, N.; Navon, N.; Glickman, Y.; Ozeri, R. Measurement of the magnetic interaction between two bound electrons of two separate ions. *Nature* **2014**, *510*, 376–380.
115. Karshenboim, S.G. Constraints on a long-range spin-dependent interaction from precision atomic physics. *Phys. Rev. D* **2010**, *82*, 113013.
116. Ji, W.; Chen, Y.; Fu, C.; Ding, M.; Fang, J.; Xiao, Z.; Wei, K.; Yan, H. New Experimental Limits on Exotic Spin-Spin-Velocity-Dependent Interactions by Using SmCo_5 Spin Sources. *Phys. Rev. Lett.* **2018**, *121*, 261803.
117. Kim, Y.J.; Chu, P.-H.; Savukov, I.; Newman, S. Experimental limit on an exotic parity-odd spin- and velocity-dependent interaction using an optically polarized vapor. *Nature Commun.* **2019**, *10*, 2245.
118. Bezerra, V.B.; Klimchitskaya, G.L.; Mostepanenko, V.M.; Romero, C. Constraining axion coupling constants from measuring the Casimir interaction between polarized test bodies. *Phys. Rev. D* **2016**, *94*, 035011.
119. Banishev, A.A.; Klimchitskaya, G.L.; Mostepanenko, V.M.; Mohideen, U. Demonstration of the Casimir Force between Ferromagnetic Surfaces of a Ni-Coated Sphere and a Ni-Coated Plate. *Phys. Rev. Lett.* **2013**, *110*, 137401.
120. Banishev, A.A.; Klimchitskaya, G.L.; Mostepanenko, V.M.; Mohideen, U. Casimir interaction between two magnetic metals in comparison with nonmagnetic test bodies. *Phys. Rev. B* **2013**, *88*, 155410.
121. Derbin, A.V.; Kayunov, A.S.; Muratova, V.V.; Semenov, D.A.; Unzhakov, E.V. Constraints on the axion-electron coupling for solar axions produced by a Compton process and bremsstrahlung. *Phys. Rev. D* **2011**, *83*, 023505.
122. Falk, A.L.; Klimov, P.V.; Ivády, V.; Szász, K.; Christle, D.J.; Koehl, W.F.; Gali, A.; Awschalom, D.D. Optical Polarization of Nuclear Spins in Silicon Carbide. *Phys. Rev. Lett.* **2015**, *114*, 247603.

123. Brax, P.; van de Bruck, C.; Davis, A.-C.; Mota, D.F.; Shaw, D. Detecting chameleons through Casimir force measurements. *Phys. Rev. D* **2007**, *76*, 124034.
124. Almasi, A.; Brax, P.; Iannuzzi, D.; Sedmik, R.I.P. Force sensor for chameleon and Casimir force experiments with parallel-plate configuration. *Phys. Rev. D* **2015**, *91*, 102002.
125. Klimchitskaya, G.L.; Mostepanenko, V.M.; Sedmik, R.I.P. Casimir pressure between metallic plates out of thermal equilibrium: Proposed test for the relaxation properties of free electrons. *Phys. Rev. A* **2019**, *100*, 022511.
126. Sedmik, R.I.P. Casimir and non-Newtonian force experiment (CANNEX): Review, status, and outlook. *Int. J. Mod. Phys. A* **2020**, *35*, 2040008.
127. Hinterbichler, K.; Khoury, J. Screening Long-Range Forces through Local Symmetry Restoration, *Phys. Rev. Lett.* **2010**, *104*, 231301.
128. Hinterbichler, K.; Khoury, J.; Levy, A.; Matas, A. Symmetron cosmology. *Phys. Rev. D* **2011**, *84*, 103521.
129. Elder, B.; Vardanyan, V.; Arkami, Y.; Brax, P.; Davis, A.-C.; Decca, R.S. Classical symmetron force in Casimir experiments. *Phys. Rev. D* **2020**, *101*, 064065.
130. Brax, P.; van de Bruck, C.; Davis, A.-C.; Shaw, D. Dilaton and modified gravity. *Phys. Rev. D* **2010**, *82*, 063519.
131. Ryutov, D.D.; Budker, D.; Flambaum, V.V. A Hypothetical Effect of the Maxwell-Proca Electromagnetic Stresses on Galaxy Rotation Curve. *ApJ* **2019**, *871*, 218.
132. Mattioli, L.; Frassino, A.M.; Panella, O. Casimir-Polder interactions with massive photons: Implications for BSM physics. *Phys. Rev. D* **2019**, *100*, 116023.
133. Kroff, D.; Malta, P.C. Constraining hidden photons via atomic force microscope measurements and the Plimpton-Lawton experiment. *Phys. Rev. D* **2020**, *102*, 095015.
134. Weinberg, S. The cosmological constant problem. *Rev. Mod. Phys.* **1989**, *61*, 1–23.
135. Frieman, J.A.; Turner, M.S.; Huterer, D. Dark Energy and the Accelerating Universe. *Annu. Rev. Astron. Astrophys.* **2008**, *46*, 385–432.
136. Zel'dovich, Ya.B. The cosmological constant and the theory of elementary particles. *Uspekhi Fiz. Nauk* **1968**, *95*, 209–230; Translated: *Sov. Phys. Usp.* **1968**, *11*, 381–393.
137. Lifshitz, E.M. The theory of molecular attractive forces between solids. *Zh. Eksp. Teor. Fiz.* **1955**, *29*, 94–110; Translated: *Sov. Phys. JETP* **1956**, *2*, 73–83.
138. Dzyaloshinskii, I.E.; Lifshitz, E.M.; Pitaevskii, L.P. The general theory of van der Waals forces. *Usp. Fiz. Nauk* **1961**, *73*, 381–422; Translated: *Adv. Phys.* **1961**, *10*, 165–209.
139. Leonhardt, U. Lifshitz theory of the cosmological constant. *Ann. Phys. (N.Y.)* **2019**, *411*, 167973.
140. Mostepanenko, V.M.; Klimchitskaya, G.L. Whether an Enormously Large Energy Density of the Quantum Vacuum Is Catastrophic. *Symmetry* **2019**, *11*, 314.
141. Mostepanenko, V.M. Some remarks on axion dark matter, dark energy and energy of the quantum vacuum. *Int. J. Mod. Phys. A* **2020**, *35*, 2040036.
142. Brax, P.; Davis, A.-C. Atomic interferometry test of dark energy. *Phys. Rev. D* **2016**, *94*, 104069.
143. Brax, P.; Davis, A.-C. Casimir, gravitational, and neutron tests of dark energy. *Phys. Rev. D* **2015**, *91*, 063503.

